3A.8

ASSIMILATION OF ICE THICKNESS INFORMATION INTO A SEA ICE MODEL

R. W. Lindsay*
Polar Science Center, Applied Physics Laboratory
University of Washington, Seattle, Washington

1. INTRODUCTION

The assimilation of observations of ice-thickness, ice-concentration, and open-water fraction into an ice thickness model offers a number of opportunities and challenges. The opportunities include the chance to correct model calculations with observations of the actual ice cover so that the model state remains closer to the true state, not only in regards to ice thickness, but in other parameters as well. The challenges include finding methods of assimilating the observations that are consistent with both the errors in the observations as well as those of the model. The observations might include only the ice concentration (from passive microwave or higher resolution visible and thermal sensors), the mean thickness (from radar altimeters), the thickness distribution of thin ice (from AVHRR or aircraft measurements), or the full thickness distribution (from upward looking sonars mounted on buoys or submarines). This paper discusses data assimilation issues and techniques and shows results of assimilation procedures on the evolution of the ice thickness distribution in the vicinity of the SHEBA ice camp.

All assimilation schemes depend on estimates of both measurement errors and model errors. With limited validation data available, the model-error characteristics are difficult to assess, yet assumptions about these errors have a profound impact on the results of assimilation procedures.

Some interesting issues arise with assimilation of ice-thickness or open-water observations because the thickness is represented by a probability distribution function (PDF). A change in the fractional area of any one thickness or bin must change the fractions of one or more of the other bins in the distribution. While assimilation is often as much art as science, it is possible to formulate a method that relies strictly on the error covariance properties of the model and the observations. The method can, however, lead to strange results because the error-covariance structure of the model is poorly understood.

The model error covariance depends on the sources of the errors. Errors in the model ice-thickness distribution can arise from errors either in the forcing parameters or in the model physics. Without extensive validation data, disentangling the two is difficult at best. First, let's consider observations of just the open-water fraction and errors in the forcings. If the prescribed divergence rates are incorrect, any discrepancy in the model and observed open-water fraction might be best understood as arising from an incorrect estimation of the divergence, and any adjustments in the distribution should be shared equally by all elements of the distribution. For example, if the observed open-water fraction is less than what is estimated by the model, the revised model estimate of the open water should be reduced, and all other classes should be increased in proportion to their fractional areas and the size of the discrepancy. Because the area of thick ice is increased, the estimated mean thickness increases, which can be substantial if the discrepancy is large. On the other hand, if it is assumed that the discrepancy comes from incorrect thermal forcing parameters or growth-rate calculations, it may make better sense to modify the thinnest part of the distribution, creating ice just at the thin end of the distribution and thereby minimize the changes in the mean ice thickness. Another alternative is to create ice of a single thickness in the model, a thickness that would be thick enough to persist during the melt season and hence provide a good match to subsequent observations of open water. This would both minimize the changes in the model ice volume and the jumps in the model open-water fraction. This last alternative was used to assimilate open-water observations at the SHEBA ice camp.

In some assimilation procedures it is useful to run the model in reverse so that the influence of observations can be included for times before the observations were made. This usually requires a linear model and, even more, reversible physical processes. Unfortunately the ridging process in sea ice is not reversible. There is no single way to take ridged ice and estimate the thickness of the ice that was crushed to form the ridge when a closing event is changed to an opening event in time reversal.

For SHEBA, observations were made by submarine, aircraft, and satellite to estimate the open-water fraction, the thin-ice portion of the thickness distribution, or the full distribution. The assimilation procedures used here depend heavily on an assessment of the errors of both the model and the observations. These errors are often poorly known and require some broad assumptions, but

* *Corresponding author's address:*
Ronald W. Lindsay, Polar Science Center, University of Washington, 1013 NE 40th St., Seattle WA 98105; e-mail: lindsay@apl.washington.edu

the method may prove increasingly useful as these errors are better quantified. Each time ice observations are assimilated into the model, ice must be created or removed to account for the new information. The resultant change in the ice volume is a measure of the agreement between the observations and the model and can serve as a validation (or repudiation) of the model calculations.

2. AN ASSIMILATION PROCEDURE

This assimilation procedure begins with estimates of the thickness distribution for some set of common thickness categories. The model and observed fractions are merged with a procedure related to the Kalman Filter (KF) (Dee, 1991; Thomas and Rothrock, 1993). Let **F** be a column vector of length n_h consisting of the fractional area coverage of each thickness bin from the model, $g_{mod}(h_i)$. Let $\mathbf{P}_F$ be the (n_h x n_h) error-covariance matrix for **F** and let **Z** be the vector of observed fractions, $g_{obs}(h_i)$, with measurement-error-covariance matrix $\mathbf{R}_Z$. In order to account for the hard constraint limiting the fractional areas to a probability distribution function, an additional pseudo-measurement is added to the observation vector that represents the sum of all the fractions. This sum must be exactly 1 and the error zero. The observation vector is estimated from the model values of g with a linear operator. This estimate is

$$\hat{\mathbf{Z}} = \mathbf{H}\mathbf{F} \quad (1)$$

For example, if n_h = 3,

$$\mathbf{H} = \begin{bmatrix} 1 & 0 & 0 \\ 0 & 1 & 0 \\ 0 & 0 & 1 \\ 1 & 1 & 1 \end{bmatrix} \quad (2)$$

where the final row of ones accounts for the pseudo-measurement. The measurement-error-covariance matrix is

$$\mathbf{R}_z = \begin{bmatrix} \varepsilon_{ow}^2 & 0 & 0 & 0 \\ 0 & \varepsilon_2^2 & 0 & 0 \\ 0 & 0 & \varepsilon_3^2 & 0 \\ 0 & 0 & 0 & 0 \end{bmatrix} \quad (3)$$

where $\varepsilon_{ow}{}^2$ is the open-water error variance and $\varepsilon_i{}^2$ are the error variances of the other categories. If only the open-water fraction is observed, the errors for the other categories are set to large numbers. For simplicity, the errors are assumed to be independent, but in fact there may be significant correlations due to the PDF constraint. The KF update step yields a refined estimate of the area fractions, the vector **G**. It is based on the difference between the observations and the model-based estimate of the observations,

$$\mathbf{G} = \mathbf{F} + \mathbf{K}(\mathbf{Z} - \hat{\mathbf{Z}}). \quad (4)$$

The Kalman gain matrix is

$$\mathbf{K} = \mathbf{P}_F\, \mathbf{H}^T [\mathbf{H}\, \mathbf{P}_F\, \mathbf{H}^T + \mathbf{R}_Z]^{-1} \quad (5)$$

and the estimate of the error-covariance matrix of the new model values is updated by

$$\mathbf{P}_G = (\mathbf{I} - \mathbf{K}\mathbf{H})\, \mathbf{P}_F \quad (6)$$

where **I** is the identity matrix. Equation (4) shows that the updated ice thickness distribution vector **G** is a weighted combination of the first guess vector **F** and the measurement vector **Z**.

Many of the observations are of the open-water fraction only. The simplest method of dealing with these observations is to determine the new open-water fraction as a weighted sum of the model and the observation values

$$g(0) = \frac{\left[\frac{g_{mod}(0)}{\varepsilon_{mod}^2(0)} + \frac{g_{obs}(0)}{\varepsilon_{obs}^2(0)}\right]}{(\varepsilon_{mod}^2(0) + \varepsilon_{obs}^2(0))} \quad (7)$$

for which a value of $\varepsilon_{mod}(0)$ = 0.01 was used. If the model fraction of open water was less than the observed, the thinnest ice was removed to accommodate the increased open-water fraction. If the model open-water fraction was larger than the observed, ice of a single thickness of 0.5 m was created in the model. This thickness was found to provide good continuity in the model for the fraction of open water from one observation to the next (Figure 1).

3. MODEL RESULTS FOR SHEBA WITH AND WITHOUT DATA ASSIMILATION

Six different observational surveys of ice thickness or open water were used in this analysis (Table 1). These surveys were made by submarine, aircraft, and satellite and varied widely in their methods and accuracy. Details may be found in the references or in Lindsay (2001b).

The thermodynamic model has 7 vertical levels for the temperature profile. The thickness distribution is determined with up to 100 characteristics. Redistribution of ice caused by deformation was included (Thorndike et al., 1975) and the deformation was determined from buoys, AVHRR, SSMI, and RGPS ice tracking (Lindsay, 2001a), not from a dynamic model. The model is more fully described in Lindsay (2001b).

The evolution of the mean ice thickness, total ice volume, and the open-water fraction are shown with and without data assimilation in Figure 1. The mean thickness and the total ice volume show little net change. Most of the open-water measurements had relatively low uncertainty, so the model estimates were forced to match the measurements. In general, the observations indicated less open water or thin ice than was represented in the model so that the assimilation procedures increased the amount of ice. This was most evident in

TABLE 1. Observations of the ice thickness or open water near SHEBA

Platform	Dates	Length or area	Notes
USS Archerfish (SCICEX)	30 September 1997	1300 km	full distribution, $\bar{h}$ = 1.54 m
Twin Otter, 5 flights	14 October 1997 to 29 March 1998	670 km average	ice thickness 0.0 to 0.5 m (Lindsay and Stern, 1999)
NCAR C-130, 7 flights	11 to 20 May 1998	1555 to 3386 km^2	open-water fraction, AMIR (Tschudi et al., 2001a)
Helicopter, 14 flights	17 May to 4 October 1998	145 km^2 average	open-water fraction, 35 mm camera (Perovich et al., 2001)
Satellite (USNR)	18 June 1998	57 km^2	open-water fraction, photo (Perovich et al., 2001)
NCAR C-130, 5 flights	8 to 26 July 1998	8.6 km^2 average	open-water fraction, video (Tschudi et al., 2001b)

June and July, but an observation in August showed more open water than the model estimates and consequently the ice volume decreased. The overabundance of open water in the model in June and July would indicate that either the melt rates for thin ice were too high or that more convergence occurred during this period than was estimated from the ice displacement measurements. The use of a nominal 0.5 m for ice created in assimilation has largely, but not entirely, smoothed the model open-water fraction.

The evolution over the year of the multiyear ice, new smooth ice, new ridged ice, and open-water fractions are shown in Figure 2. Also shown are the mean thickness of each of the categories and the overall mean thickness. According to the model, the mean thickness increased from 1.54 m to 3.56 m over the year, in spite of more melt than growth for ice over 1 m thick. This occurred because of the net convergence experienced by the pack in the vicinity of the ship. This convergence caused a large ridged-ice fraction, about one-half of the area at the end of the year, and removed all of the new smooth ice into ridges. The mean thickness of the new ridged ice was over 5 m by the end of the experiment.

Data assimilation in this exercise had the greatest influence on the open-water fraction, in that assimilation restrained model overestimation of the open water during the summer months. The observations of the thin-ice distribution in the fall and winter had minor influences on the mean ice thickness and served to verify the model prediction of the small fraction of thin ice present. The methods described here can be applied to wider regions, but, as always, understanding the model errors will be the key to a successful effort.

Acknowledgements: I would like to thank our colleagues in the SHEBA Atmospheric Surface Flux Group, the SHEBA Snow and Ice Studies Group, the SHEBA Project Office, the Atmospheric Radiation Measurement Program, the NCAR C-130 team, the Polar Remote Sensing Group at JPL, and the Polar Science Center SCICEX group for a wide variety of data used in this study. This work has been funded by the National Science Foundation under the Arctic System Science Program.

REFERENCES

Dee, D.P., 1991: Simplification of the Kalman filter for meteorological data assimilation. *Q. J. R. Meteorol. Soc.*, **117**, 365–384.

Lindsay, R. W., 2001a: Ice deformation near SHEBA. *J. Geophys. Res.*, in press.

Lindsay, R. W., 2001b: Ice thickness distributions near SHEBA. *J. Geophys. Res.*, submitted.

Lindsay, R. W. and H. L. Stern, 1999: Aircraft-based estimates of thin-ice fraction near SHEBA. *Proceedings of the Fifth Conference on Polar Meteorology and Oceanography*, Amer. Meteorol. Soc., 15-20 January 1999, Dallas TX, 118-123.

Perovich, D. K., W. B. Tucker III, and K. A. Ligett, 2001: Aerial observations of the evolution of ice surface conditions during summer. *J. Geophys. Res.* in press.

Thomas, D.R., and D.A. Rothrock, 1993: The Arctic Ocean Ice Balance: A Kalman Smoother Estimate, *J. Geophys. Res.*, **98**(C6), 10053–10067.

Thorndike, A. S., D. A. Rothrock, G. A. Maykut, and R. Colony, 1975: The thickness distribution of sea ice. *J. Geophys. Res.*, **80**, 4501–4513.

Tschudi, M. A., J. A. Curry, and J. A. Maslanik, 2001a: Characterization of springtime leads in the Arctic Ocean from airborne observations during FIRE/SHEBA, *J. Geophys. Res*. in press.

Tschudi, M. A., J. A. Maslanik, and J. A. Curry, 2001b: Airborne observations of summertime surface features and their effect on surface albedo during SHEBA. *J. Geophys. Res.*, in press.

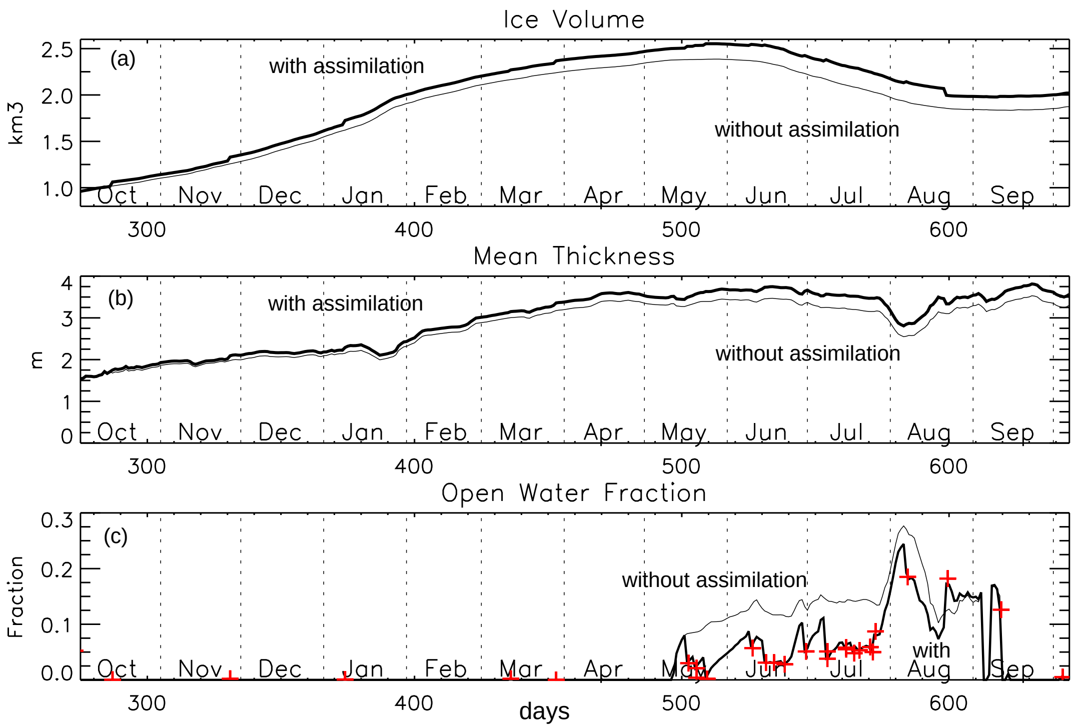

FIG. 1. Time series comparing runs with and without data assimilation of ice thickness and open water observations during SHEBA: (a) the total ice volume in the cell centered on the camp with an initial area of 625 km^2, (b) the mean ice thickness, and (c) the open-water fraction. The crosses indicate observations of the open-water fraction.

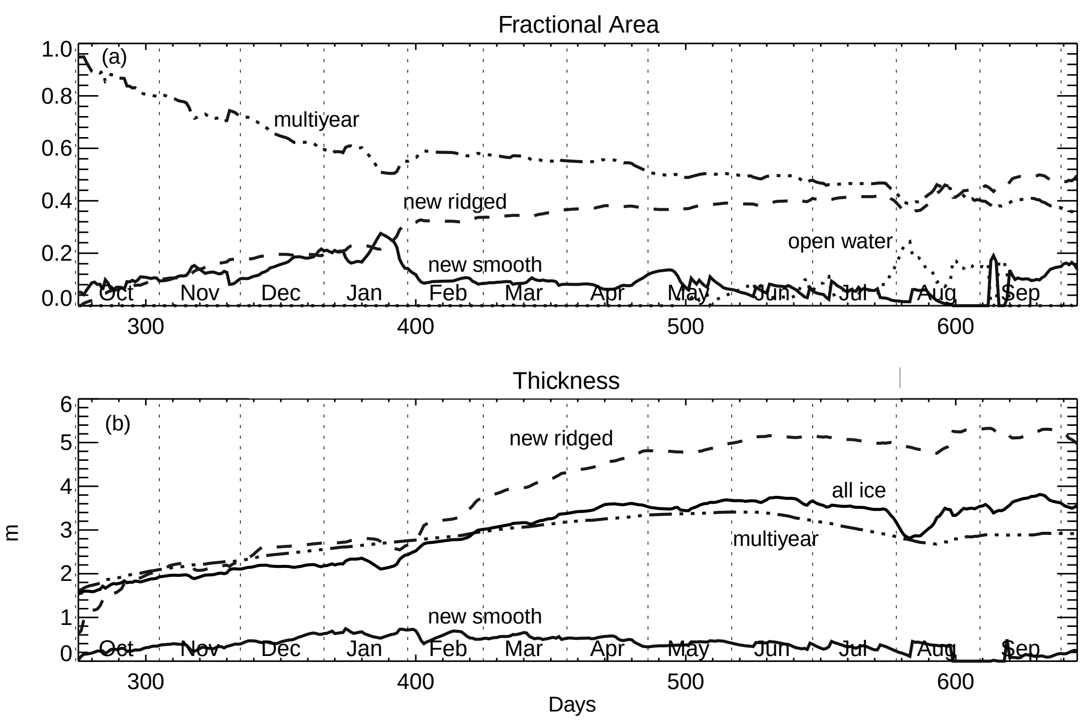

FIG. 2. Area fraction (a) and mean thickness (b) of multiyear ice, new smooth ice, new ridged ice, and open water at the SHEBA ice camp, 2 October 1997 to 12 October 1998.